

Field-emission characterization of the 10×10 singly addressable double-gated polysilicon tip array

N. N. Chubun,^{a)} A. G. Chakhovskoi, M. Hajra, and C. E. Hunt

Electrical and Computer Engineering Department, University of California, Davis, California 95616

(Received 5 April 2002; accepted 24 June 2002; published 4 February 2003)

Polysilicon-on-insulator singly addressable arrays, consisting of double-gated field-emission cells, were fabricated and tested. The field-emission tips were formed by a subtractive technique, using an array of ten polysilicon stripes on the insulating substrate. The stripe structure was oxidized for dielectric isolation and coated with a second polysilicon layer as an extracting gate electrode. The polysilicon layer was then oxidized to provide a second isolation layer for separation from a top gold film, deposited as a focusing electrode. Finally, an 1.7 μm aperture was opened, using wet buffered etching of the silicon dioxide. The structure allows us to address electrically a single tip at the intersection of any cathode row and extracting gate column. A focusing voltage could be applied independently to the second gate of any tip during operation to focus the electron flux of an operating tip. The focused array may be suitable for multi-beam electron lithography application and new generation of data storage devices. © 2003 American Vacuum Society.

[DOI: 10.1116/1.1527634]

I. INTRODUCTION

A conventional field-emission cell, which usually consists of an emission tip surrounded by a small aperture in an extracting electrode (grid), has very complicated electron-optical characteristics. Electron beam trajectories are influenced not only by the electric field formed between the emission tip and the gate, but also by the field in the proximity of the emission site. In a multiple-cell array, the electrons emitted from a single tip at a large emission angle interfere with the electrical field generated by the neighboring cells. This problem can be effectively resolved by controlling a shape of the individual electron beams. It is possible to generate a focused or collimated electron beam by using the fringe electric field formed along the edge of the extracting grid electrode if an adjacent electrode—a focusing lens having a lower potential—is placed in the vicinity of the extraction grid. The nearly uniform accelerating field provided by an anode positioned at some macroscopic distance above the device will be distorted by the difference of the potentials between the extracting grid and the lens electrodes, producing an electrostatic focusing effect in the extended volume above the field emitters, while not significantly affecting the emission current. It has been proposed in Ref. 1 that by fabricating the lens electrodes coaxial with each tip to form an electrostatic lens system, one could persuade all the electrons emitted from every tip of the array to travel in the same direction. Several researchers^{2,3} have calculated the design parameters (spacing, aperture radii and voltages) to meet these conditions. Focusing effect can be achieved by two approaches of integrating the focusing lens to the conventional gated field-emission arrays. The first approach is a “coplanar-type” focusing.^{4–7} The focusing lens of the coplanar type is located around the gate electrode surrounding an emissive tip in the same plane. The other ap-

proach utilizes a vertical arrangement of an extraction and a focusing electrode resulting in coaxial focusing.^{8–11} [A schematic of these arrangements is shown in Figs. 3(a) and 3(b).]

Numerical simulations have shown that the coplanar focusing can have certain advantages in comparison to the coaxial type since the electric field at the emitter tip is not affected so strongly by the coplanar lens bias, and therefore the beam current is less sensitive to the lens bias.³ It is difficult, however, to increase the packing density of the coplanar-type field-emission arrays because the focusing lenses spread widely around the emitter tips. On the other hand, the focusing effect in the case of the coaxial arrangement can be stronger than in the case of the coplanar configuration.

Most of the modern electron beam-control systems for the field-emission sources use only two focusing electrodes (grids). In the present work, we also performed an attempt to fabricate a double-gated thin-film focusing system for addressable silicon-on-insulator field-emission structures, which we have developed using subtractive technique.¹²

II. EXPERIMENT AND DISCUSSION

Briefly, the existing process of single-gated field-emission cell fabrication consists of growing of the polysilicon-on-insulator structures with the polysilicon thickness of 2.5 μm [Fig. 1(a)]. The polysilicon layer is patterned and dry etched under silicon dioxide-chromium mask resulting in the formation of emission tips [Figs. 1(b)–1(d)]. Etching process is followed by the oxidation sharpening [Fig. 1(e)] which also forms an insulation layer of silicon dioxide for a gold film, deposited as a gate electrode [Fig. 1(f)]. The cathode is ready when the masking cap is removed [Figs. 1(g) and 1(h)]. On the base of this simple and inexpensive technology we have developed a technique for double-gated field-emission cell fabrication. The technological schematic diagram of the second gate integration into a polysilicon field-emission cell is

^{a)}Electronic mail: nchubun@ece.ucdavis.edu

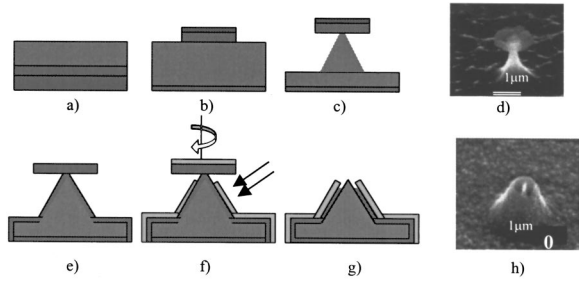


FIG. 1. Schematic process steps for single-gate field-emission cell fabrication.

shown in Figs. 2(a)–2(d). After oxidation sharpening, the structure is coated with polysilicon layer with a thickness of about 0.5 μm [Fig. 2(a)]. This layer is oxidized producing an oxide thickness up to 0.5 μm on the top of the polysilicon. The oxidation changes the size and the shape of the tip, which is illustrated by the scanning electron microscopy (SEM) micrographs [Fig. 2(b)]. The tip cup acquires an almost perfect spherical shape. This shape changes the shadowing effect of the cup, affecting the parameters of the next technological step—the deposition of the gold focusing grid [Fig. 2(c)]. The sequence of several etching steps removes the cap from the top of the structure and opens up the final emission cell [Fig. 2(d)].

It has been found during the process development that with variation of the films' thickness and the process conditions two different types of emission cells could be fabricated. The first configuration is very similar to the coaxial electron-optic type. The lens electrode is placed above the gate electrode and is separated from the gate by an insulator

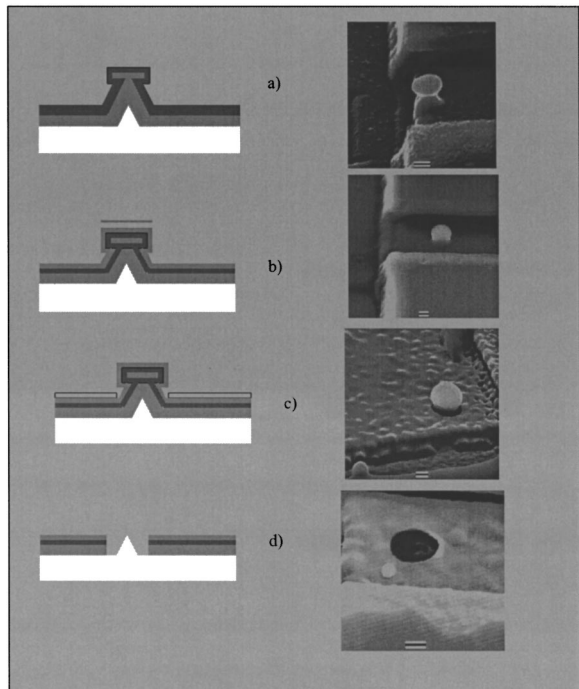


FIG. 2. Schematic diagram of the double-gated cell fabrication process.

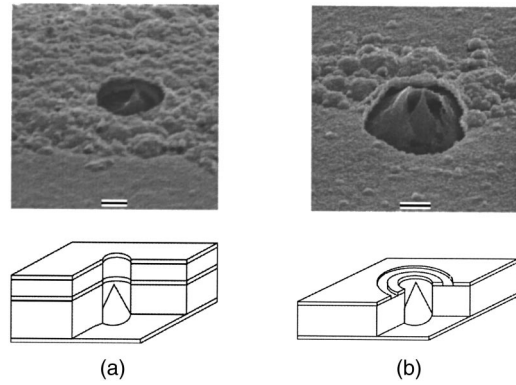


FIG. 3. Coaxial-type of focusing system (a) and coplanar-type of focusing system (b).

layer. Figure 3(a) illustrates this configuration by the SEM micrograph and the geometrical delineation. Another type of the double-gated emission cell of the coplanar type is illustrated by Fig. 3(b). These two types of double-gated cells have significant differences in electron-optical properties, but both of them can be utilized in various types of microelectronic devices.

The goal of the work is not limited by double-gated cathode cell fabrication, but also involves the design and fabrication of the 10×10 matrix test device along with the packaging suitable for vacuum chamber tests. Figure 4 shows the optical micrographs of the 10×10 field-emission matrix device. The matrix consists of ten vertical polysilicon stripes as cathode columns, and two layers of grid rows. The cathode columns have contact pads on both (upper and lower) ends, which is necessary for resistivity control. Contact pads for polysilicon extracting grids are located on the left side of the chip, and for the focusing gold grids on the right side. The actual size of the matrix is 500 μm, with each stripe of 34 μm in width and 16 μm gap between them. The measured cathode line resistance was about 1 MΩ, extracting grid stripe resistance was nearly 200 kΩ, and gold stripe resistance did not exceed 6 Ω. Polysilicon technology is able to provide an extremely wide range of built-in resistances for individual cathodes by simply changing the doping level of the polysilicon.

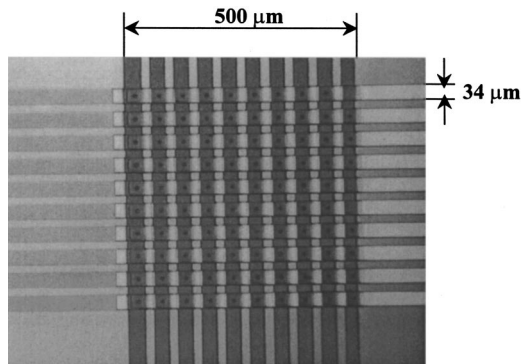


FIG. 4. Optical micrograph (30×) of the 10×10 matrix of the test device.

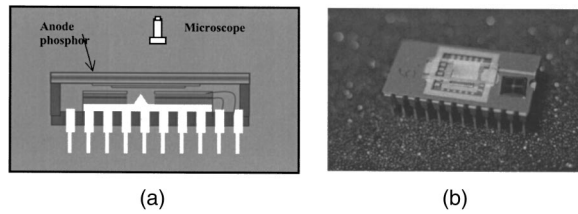


FIG. 5. Tetrode structure for visual and electric testing of the double-gated field-emission array (a) and the micrograph of the test device package.

To test the matrices, the tetrode package for the visual and the electrical testing of the double-gated field-emission arrays was designed. The package, shown in Fig. 5(a), consists of a ceramic integrated circuit carrier with 24 electric leads, a conductive phosphor screen used as an anode, and a cathode matrix. Most of the grid and cathode stripes of the test device were connected with carrier leads by the gold wire bonding. To improve optical resolution of the focused image, the phosphor screens were made using electrophoretical deposition of very fine low voltage phosphor powder with particle size less than $1 \mu\text{m}$ onto glass slides coated with conductive indium tin oxide. Figure 5(b) shows an actual view of the test package. The test chip with the field emission matrix is placed at the top of the carrier to provide a reference scale. The external size of the chip is $5 \times 5 \text{ mm}$. The triode and addressing characteristics of the samples of 10×10 matrix were published in our earlier work.¹²

One of the preliminary results of focusing electrode influence on electron beam shape is shown in Fig. 6. To provide a fair comparison, the focusing measurements were performed at constant anode current of 80 nA in dc mode for coaxial grid arrangement. The diameter of the observed light spot changes following the variation of the second gate voltage under constant anode current. In Fig. 6(a) diffused spot of light of 2–2.5 mm in diameter is obtained under the same positive potential for the extracting and the focusing grids. The extracting and the focusing grid potentials were set to

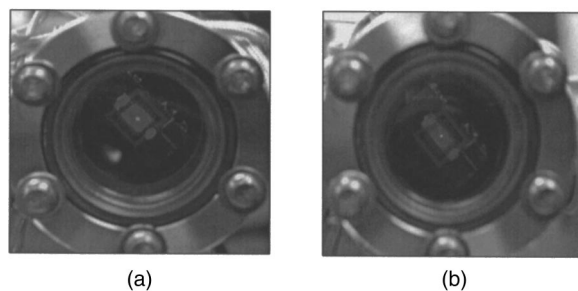


FIG. 6. Focusing at various terminal voltages and constant anode current 80 nA. (a) Extracting and focusing grid potential +215 V anode voltage +500 V, (b) extracting grid under +230 V focusing grid grounded, anode voltage +800 V.

215 V; the anode voltage was 500 V. This condition is similar to the electron optics of a single-gated cell. In Fig. 6(b) a sharp and bright focused spot with the diameter of $\sim 0.6 \text{ mm}$ is obtained as a result of applying the ground potential (which is equal to the cathode potential) to the focusing grid. Under this condition the extracting grid voltage had to be increased to 230 V, and the anode voltage had to be increased to 800 V to keep the anode current constant. A visual linear size of the focused light spot was reduced by a factor of 4. We consider this observation as a promising result demonstrating a proof of principle for the proposed focusing technique. More detailed characterization of the focusing action will require a substantial modernization of the experimental setup.

III. CONCLUSION

- (1) Double-gated focused field-emission arrays fabrication technology has been developed on the base of polysilicon-on-insulator structure and subtractive technology.
- (2) Both coaxial and coplanar double-gated focusing structures can be fabricated with minor variation of thin film thickness.
- (3) The design of the field-emission cathode matrix with a wide range of the built-in loading resistors and two independent gate electrodes was developed and tested.
- (4) Significant focusing effect was experimentally observed under constant anode current conditions.

ACKNOWLEDGMENTS

The authors acknowledge the helpful input of Dr. Si-Ty Lam, Dr. Jim Brug and colleagues of Hewlett-Packard labs. This work was funded through the DARPA-MTO MEMS program under Contract No. F30602-98-3-0232, administered by the U.S. Air Force Material Command.

¹D. L. Fraser, U.S. Patent No. 3,753,022.

²I. I. Golenitsky, V. P. Sazonov, N. N. Chubun, and S. A. Rumyantsev, *J. Vac. Sci. Technol. B* **13**, 589 (1995).

³W. D. Kesling and C. E. Hunt, *IEEE Trans. Electron Devices* **42**, 340 (1995).

⁴C. M. Tang, T. A. Swyden, and A. C. Ting, *J. Vac. Sci. Technol. B* **13**, 571 (1995).

⁵C. M. Tang *et al.*, *J. Vac. Sci. Technol. B* **14**, 3455 (1996).

⁶K. Yokoo, M. Arai, M. Mori, J. Bae, and S. Ono, *J. Vac. Sci. Technol. B* **13**, 491 (1995).

⁷Y. Tohma, S. Kanemaru, and J. Itoh, *J. Vac. Sci. Technol. B* **14**, 1902 (1996).

⁸J. Itoh, Y. Tohma, S. Kanemaru, and K. Shimizu, *J. Vac. Sci. Technol. B* **13**, 1968 (1995).

⁹Y. Yamaoka, S. Kanemaru, and J. Itoh, *Jpn. J. Appl. Phys., Part 1* **35**, 6626 (1996).

¹⁰W. D. Kesling and C. E. Hunt, *J. Vac. Sci. Technol. B* **11**, 518 (1993).

¹¹J. H. Lee, Y. H. Song, S. Y. Kang, S. G. Kim, K. I. Cho, and H. J. Yoo, *J. Vac. Sci. Technol. B* **16**, 811 (1998).

¹²N. N. Chubun, A. G. Chakhovskoi, C. E. Hunt, and M. Hajra, *Solid-State Electron.* **45**, 1003 (2001).